

Supporting Information

Constructing unique heterogeneous cobalt-manganese oxideporous microspheres as anode for long-cycle and high-rate lithium ion batteries

Bin Wu^a, Yue Xie^a, Yaqin Meng^a, Cheng Qian^a, Yingying Chen^a, Aihua Yuan^a, Xingmei Guo^a, Hongxun Yang^{a,c,}, Shijian Wan^b, and Shengling Lin^{a,*}*

^aSchool of Environmental & Chemical Engineering, Jiangsu University of Science and Technology, Zhenjiang 212003, Jiangsu, China

^bSchool of Humanities & Sciences, Jiangsu University of Science and Technology, Zhangjiagang 215618, Jiangsu, China

^cJiangsu Tenpower Lithium Co. Ltd., Zhangjiagang 215618, Jiangsu, China

*Corresponding author: E-mail address: yhongxun@126.com (Hongxun Yang); linshl5757@sina.com (Shengling Lin).

Synthesis of (Co, Mn)(Co, Mn)₂O₄ microspheres:

In a typical procedure, 1.5 mmol CoCl₂•6H₂O, 1.5 mmol MnCl₂•4H₂O were dissolved in 40 mL ethylene glycol. 2.4 g NH₄HCO₃ were added into the above solution followed by ultrasonic 15 min to mix and dissolve. The resulting solution was then transferred to 50 mL stainless steel autoclaves with Teflon liner and then kept at 200 °C for 20 h in an oven. The product was collected by centrifugation with absolute ethanol for 4 times, and then dried at 60 °C for 12 h in a vacuum oven. The as-obtained precursors were heated in a furnace at 500°C for 3 h with a heating rate of 2 °C min⁻¹ in N₂. Finally, the (Co, Mn)(Co, Mn)₂O₄ microspheres could be obtained.

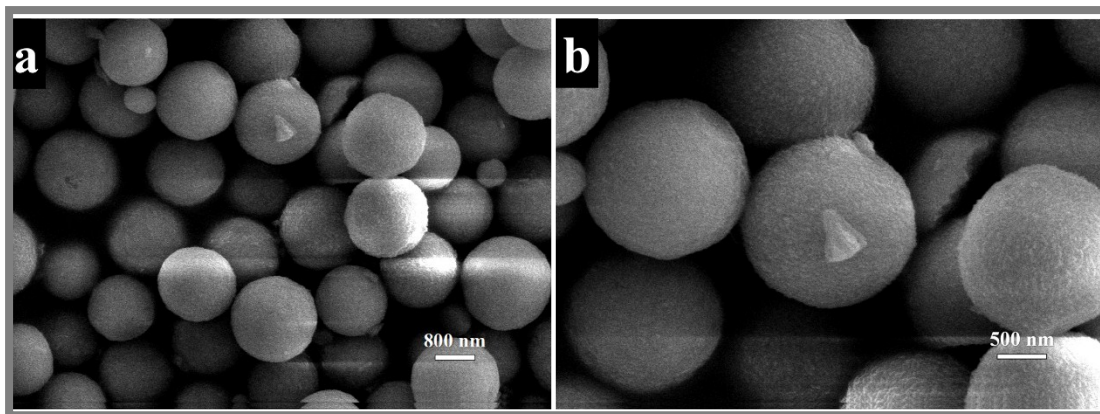


Fig. S1 (a, b) SEM images of CoMn-precursor; (c) XRD pattern of CoMn-precursor; (d) TG image of CoMn-precursor under nitrogen conditions.

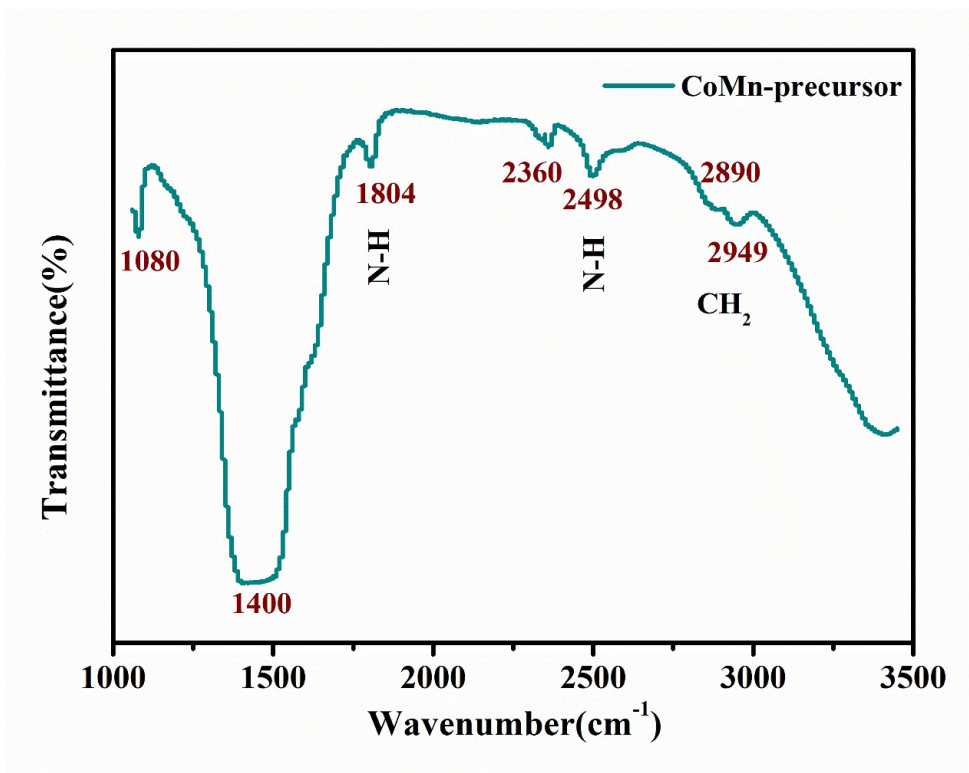


Fig. S2 FTIR spectra of the precursors of CoMn-precursor.

The peaks at 2949 and 2890 cm^{-1} confirm the presence of (CH_2) of PEG and HMT.¹ The stretching vibration and the in-plane flexural vibration of the N-H bond are observed at 2498 and 1804 cm^{-1} , respectively, which are ascribed to the HMT on the precursors.² In addition, the band near 2360 cm^{-1} is attributed to the absorbance of CO_2 on the surface of the samples, and the peaks at 1400 , 1080 , a feature of carbonate, can be ascribed to the $\text{Mn}_{0.5}\text{Co}_{0.5}\text{CO}_3$.^{3,4}

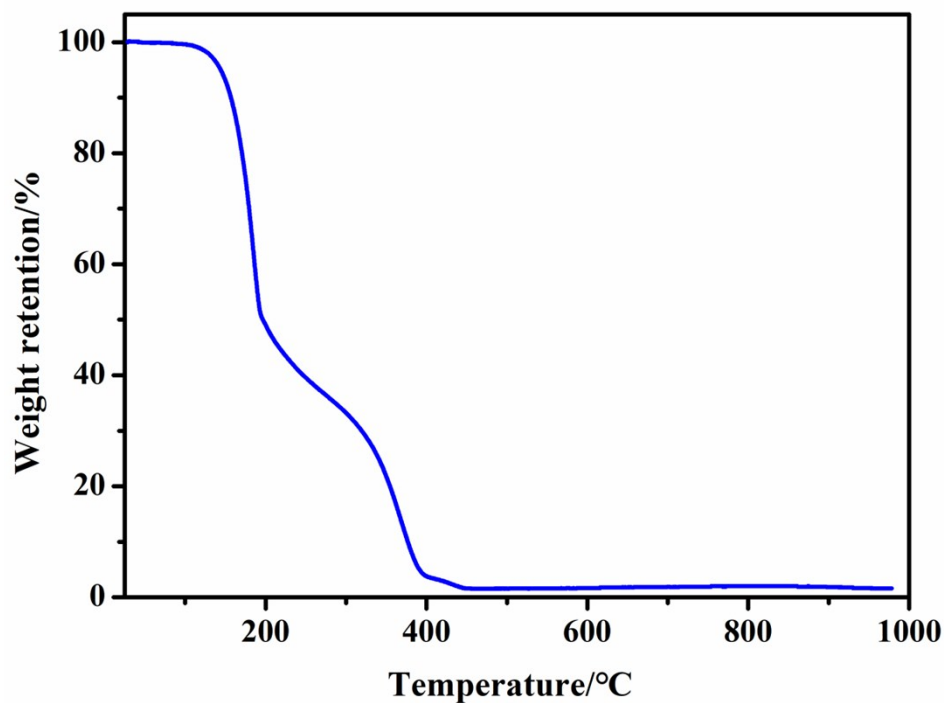


Fig. S3 TG curves of the PEG and HMT with 1:1 uniform mixed in N₂.

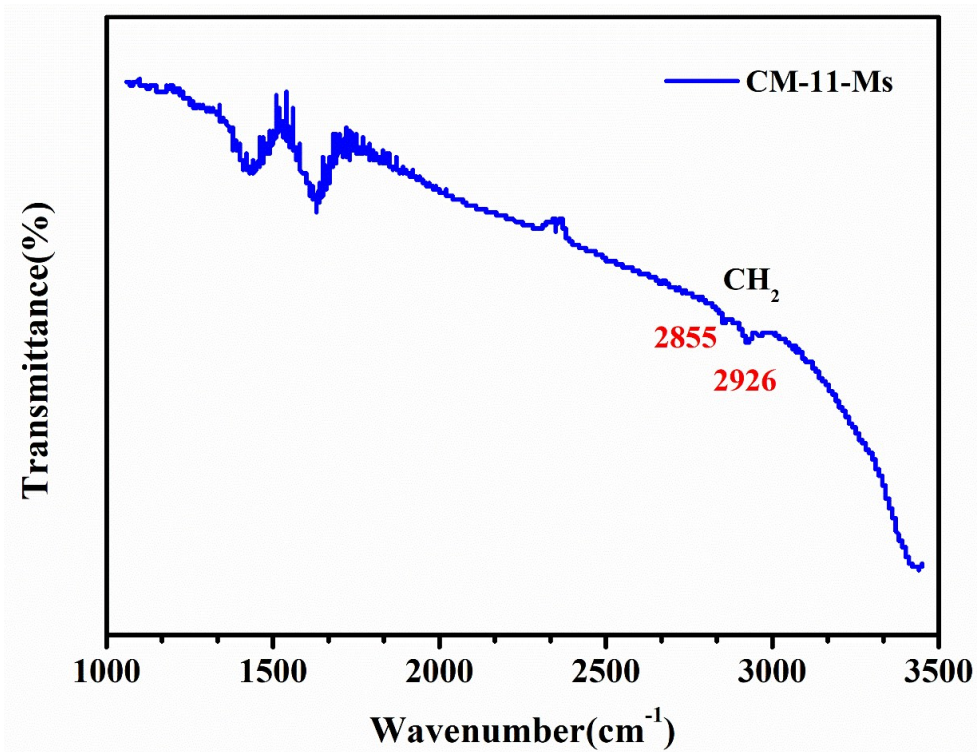


Fig. S4 FTIR spectra of the precursors of CM-11-Ms.

The peaks at 2926 and 2855 cm⁻¹ are assigned to the asymmetric and symmetric methylene stretches ($\nu_{\text{as}}(\text{CH}_2)$, $\nu_{\text{s}}(\text{CH}_2)$) of ethylene glycol and HMT.

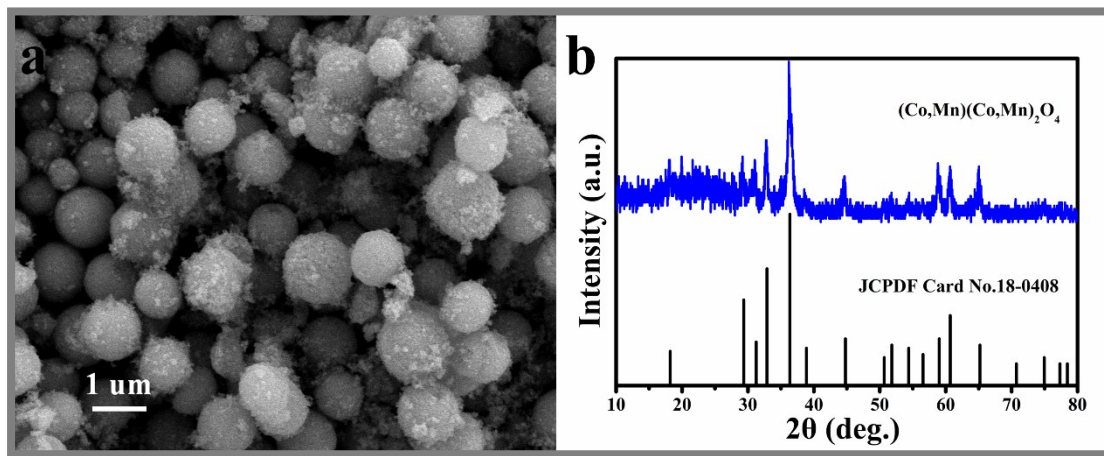


Fig. S5 (a,b) SEM images and XRD of $(\text{Co}, \text{Mn})(\text{Co}, \text{Mn})_2\text{O}_4$.

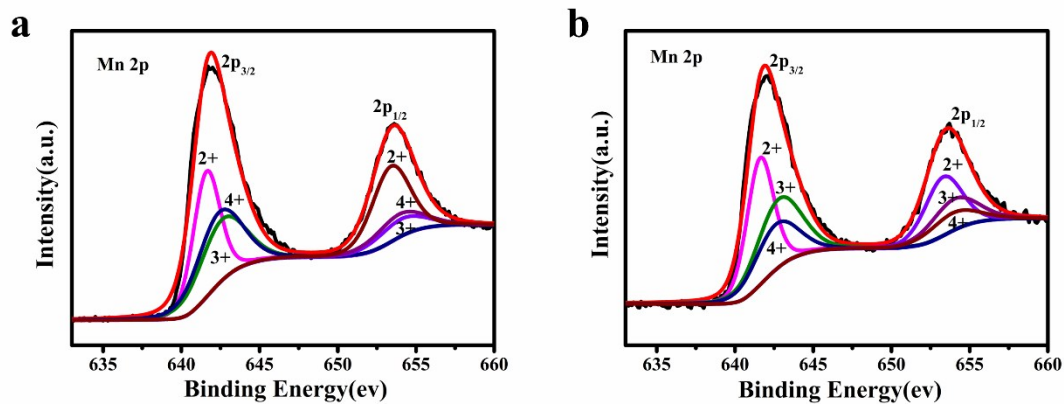


Fig. S6 XPS spectra of Mn elements of CM-11-Ms (a) and CM-11-CSMs (b).

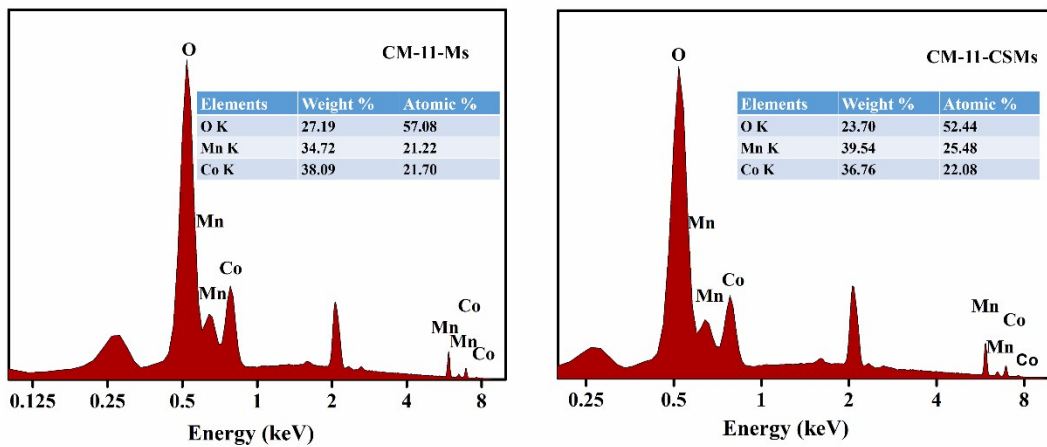


Fig. S7 EDS spectra of CM-11-Ms and CM-11-C

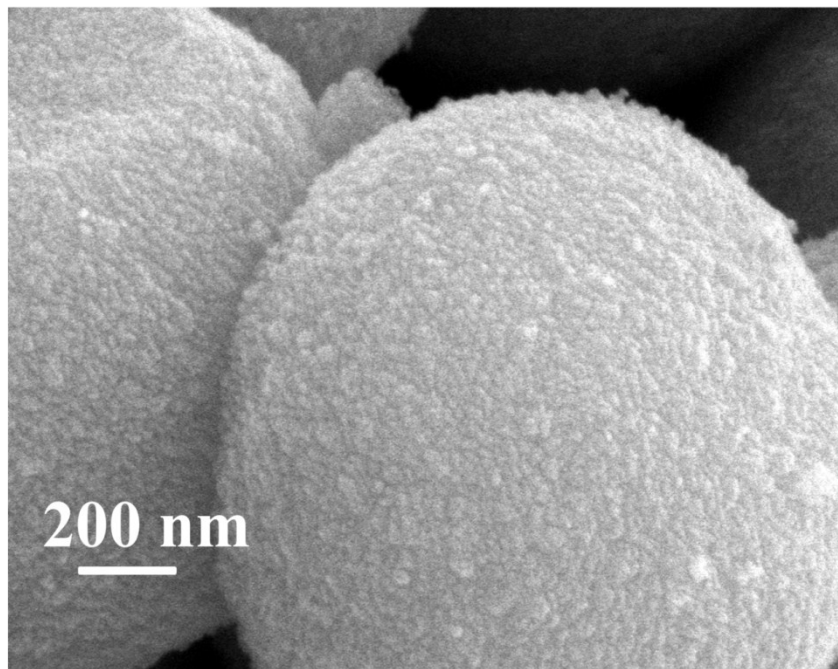


Fig. S8 SEM image of CM-11-Ms

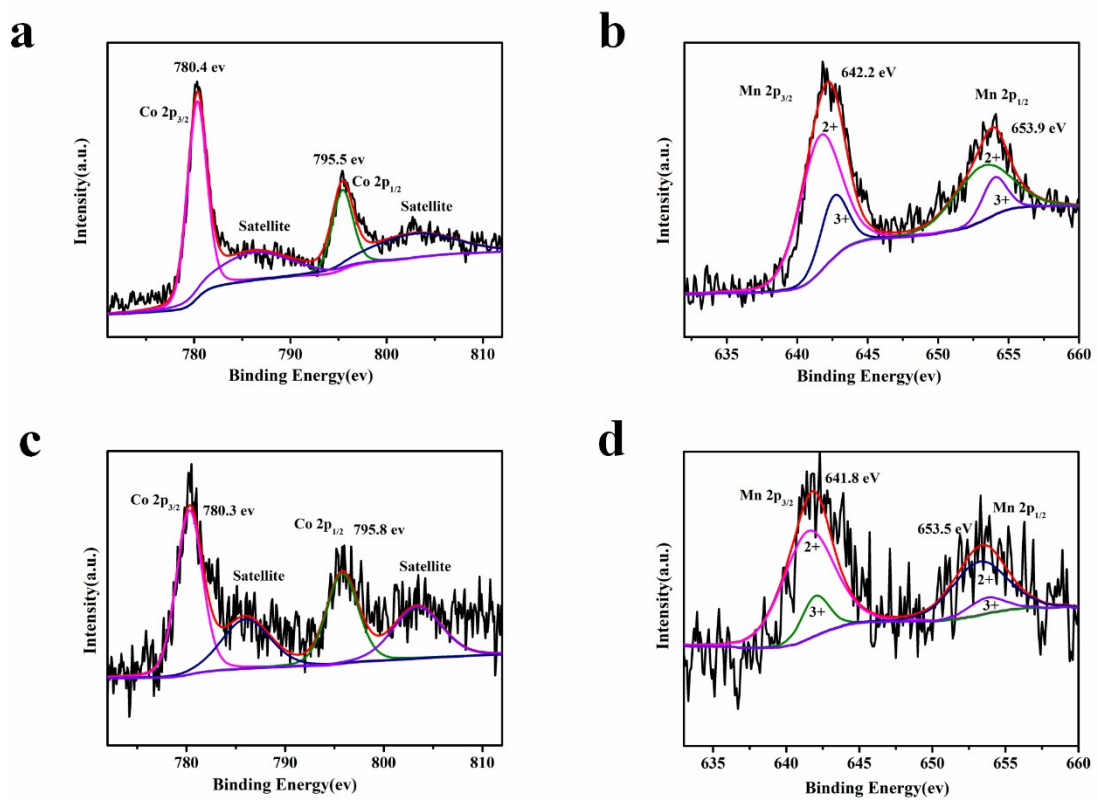


Fig. S9 XPS spectra of (a, b) CM-11-Ms and (c, d) CM-11-CSM after CV.

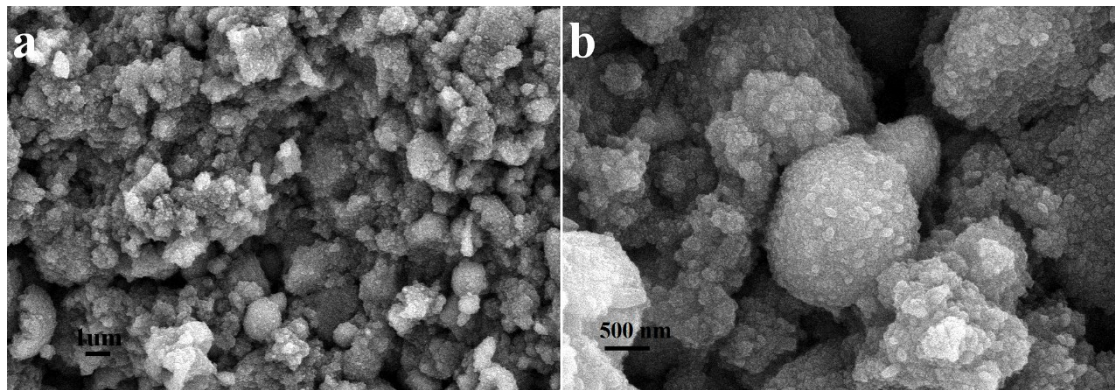


Fig. S10 SEM images of CM-11-Ms after 800thcycles at 1A g⁻¹.

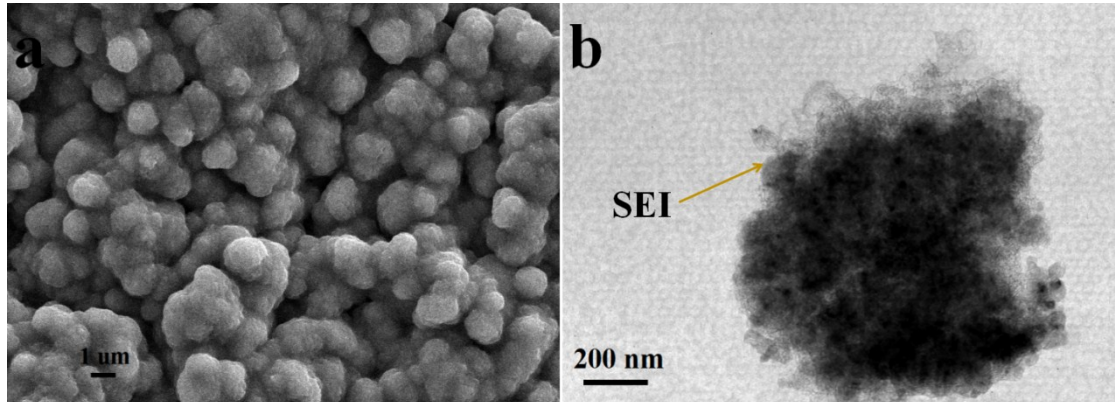


Fig. S11(a) SEM and (b)TEM images with bright field of CM-11-CSMs after 800thcycles at 1A g⁻¹.

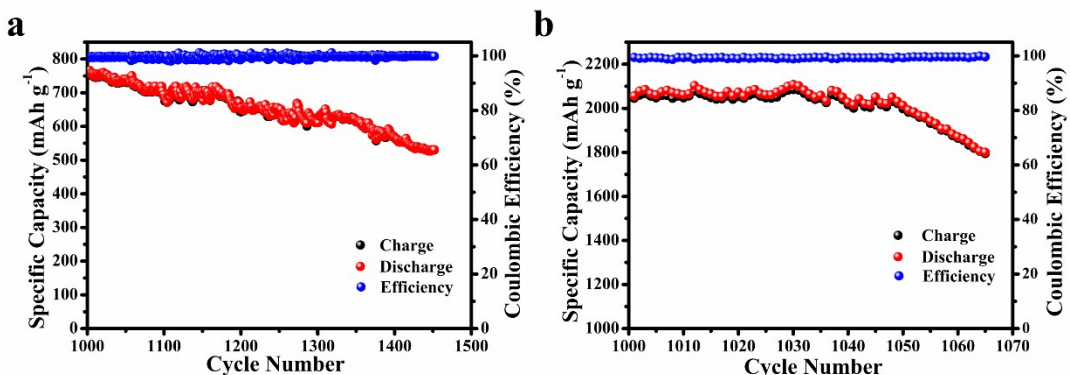


Fig. S12 Continued cycling performance of CM-11-Ms(a) and CM-11-CSM(b) after 1000cyclesat 1A g⁻¹.

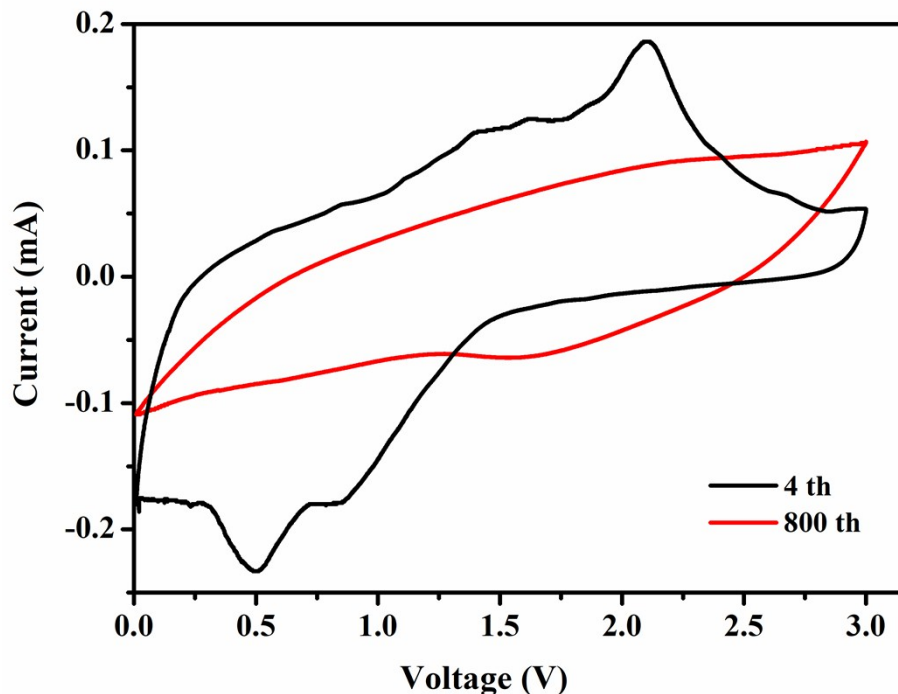


Fig. S13 Cyclic voltammograms of the 4th and 800th cycles of CM-11-Ms in a voltage range of 0.01-3.00 V at a scanning rate of 0.2 mV s⁻¹.

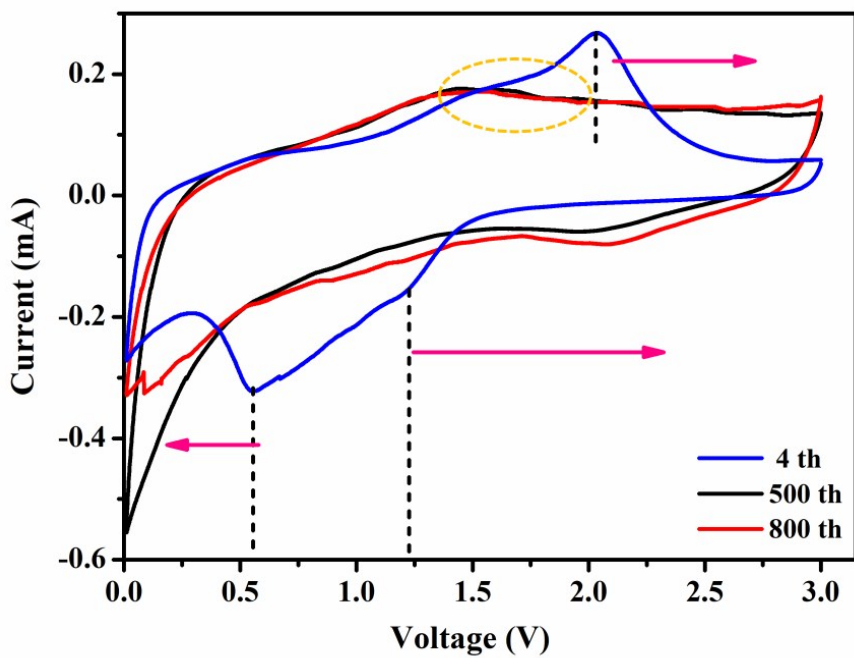


Fig. S14 Cyclic voltammograms of the 4th, 500th and 800th cycles of CM-11-CSMs in a voltage range of 0.01-3.00 V at a scanning rate of 0.2 mV s⁻¹.

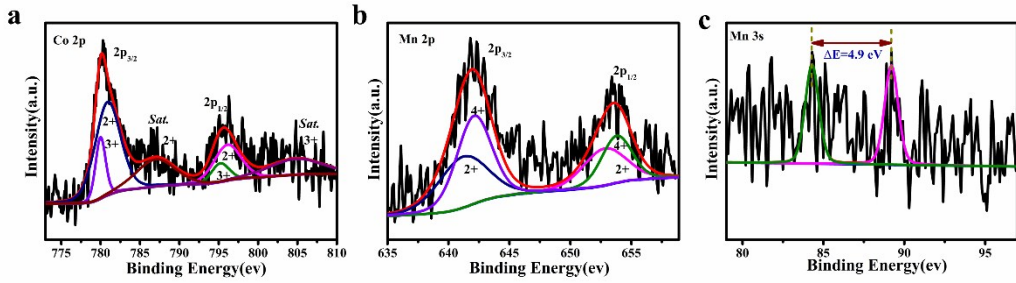


Fig. S15 XPS spectra of CM-11-CSM after 800th cycles at 1 A g⁻¹.

In the Co 2p spectrum (Fig. S15a), two peaks of Co 2p_{3/2} and Co 2p_{1/2} are located at 780.2 and 795.6 eV and two conspicuous shake-up satellite peaks are located at 787 and 804.8 eV, respectively, revealing the co-existence of Co²⁺ and Co³⁺.⁵ As shown in Fig. S15b and 15c, two characteristic peaks of Mn 2p 1/2 and 2p 3/2 at about 653.6 and 642 eV were observed, and the peak splitting amplitude of the Mn 3s spectrum was 4.9 eV, indicating the presence of Mn²⁺ and Mn⁴⁺.⁶

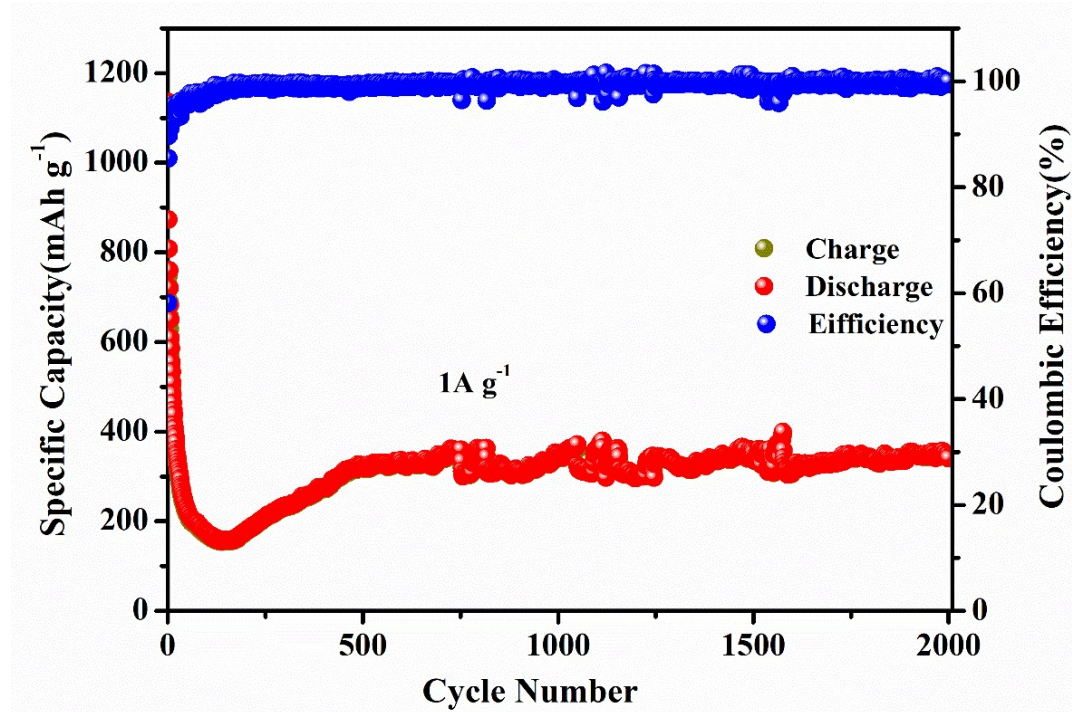


Fig. S16 Continued cycling performance of (Co, Mn)(Co, Mn)₂O₄ at 1 Ag⁻¹.

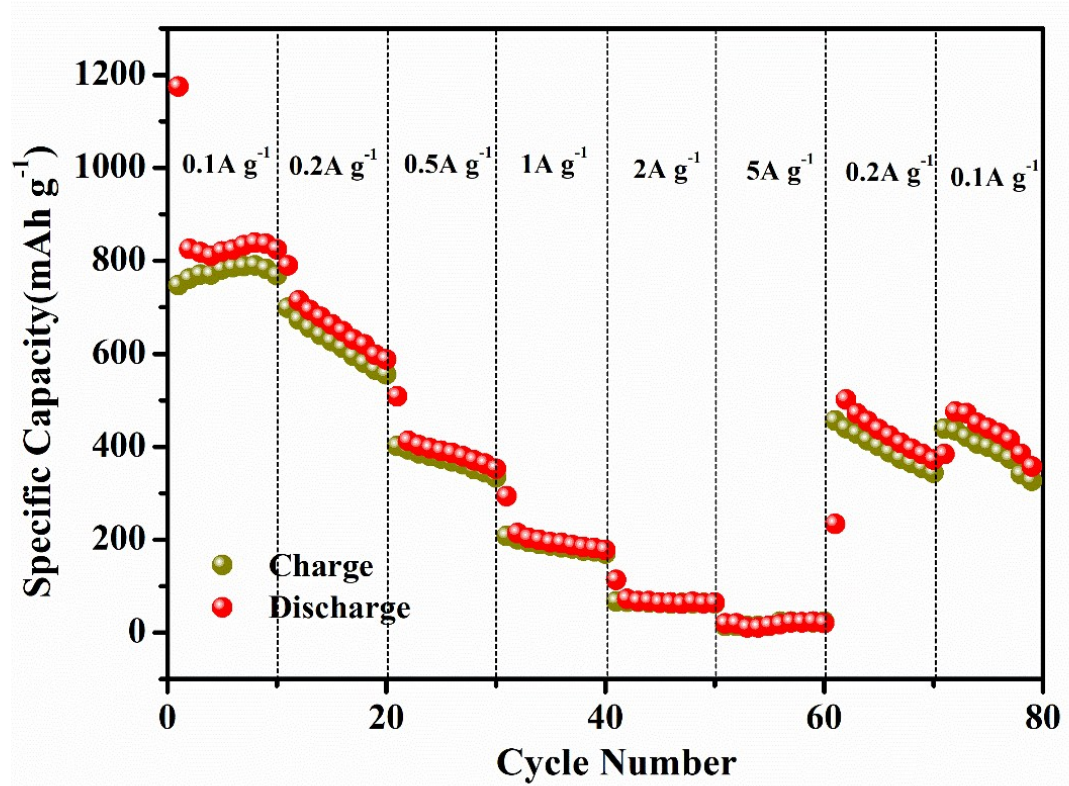


Fig. S17 Rate performance at different rates of CM-11-Ms.

Table S1 Comparison of electrochemical properties for Co-Mn binary metal oxides, single MnO and Co₃O₄ metal oxides as anodes for lithium ion batteries.

Samples	Current density (mA g ⁻¹)	Cycle number	Reversible capacity (mAh g ⁻¹)	Ref.
CM-11-Ms	1000	1000	745	This work
CM-11-CSMs	1000	1000	2175.8	This work
ZnCo ₂ O ₄ nanoflakes	80	25	750	¹
Porous MnCo ₂ O ₄ and CoMn ₂ O ₄ microspheres	1000	1000	740(MnCo ₂ O ₄) 420(CoMn ₂ O ₄)	²
Nanoscale MnO on Graphene	2000	400	843.3	⁵
ZnMn ₂ O ₄ hollow microspheres	400	100	772	⁷
CoMn ₂ O ₄ hollow nanofibers	400	50	526	⁸
Mn ₃ O ₄ nano-octahedra	50	50	500	⁹
RGO-ZnMn ₂ O ₄ nanorods	100	50	707	¹⁰
ZnCo ₂ O ₄ yolk-shelled microspheres	1000	500	331	¹¹
NiCo ₂ O ₄ porous microrods	500	600	719	¹²
Co ₃ O ₄ snowflake-shaped	500	100	1044	¹³
Spinel Mn _{1.5} Co _{1.5} O ₄ core-shell microspheres	400	300	618	¹⁴
Co ₃ O ₄ mesoporous microdisks	100	30	749	¹⁵
ZnMn ₂ O ₄ Ball-in-Ball Hollow Microspheres	400	120	750	¹⁶
Monodisperse NiCo ₂ O ₄ mesoporous microspheres	800	500	705	¹⁷
Co ₃ O ₄ hollow sphere	1000	850	927	¹⁸
CoMn ₂ O ₄ nanomaterials	325	1000	624	¹⁹
Double-Shelled CoMn ₂ O ₄	200	50	624	²⁰
Multiporous MnCo ₂ O ₄ and CoMn ₂ O ₄ spinel quasi-hollow spheres	200	25	755(MnCo ₂ O ₄) 706(CoMn ₂ O ₄)	²¹
CoMn ₂ O ₄ Spinel Hierarchical Microspheres	100	65	894	²²

- Y. Qiu, S. Yang, H. Deng, L. Jin and W. Li, *J. Mater. Chem.*, 2010, **20**, 4439.
- G. Li, L. Xu, Y. Zhai and Y. Hou, *J. Mater. Chem. A*, 2015, **3**, 14298-14306.
- L. Song, S. Zhang, X. Wu, Z. Wang and Q. Wei, *Chem. Eng. J.*, 2012, **195-196**, 15-21.
- P. Huang, X. Zhang, J. Wei, J. Pan, Y. Sheng and B. Feng, *Mater. Chem. Phys.*, 2014, **147**, 996-1002.
- Y. Sun, X. Hu, W. Luo, F. Xia and Y. Huang, *Adv. Funct. Mater.*, 2013, **23**, 2436-2444.

6. M. Toupin, T. Brousse and D. Bélanger, *Chem. Mater.*, 2002, **14**, 3946-3952.
7. L. Zhou, H. B. Wu, T. Zhu and X. W. Lou, *J. Mater. Chem.*, 2012, **22**, 827-829.
8. G. Yang, X. Xu, W. Yan, H. Yang and S. Ding, *Electrochimica Acta*, 2014, **137**, 462-469.
9. S. Z. Huang, J. Jin, Y. Cai, Y. Li, H. Y. Tan, H. E. Wang, G. Van Tendeloo and B. L. Su, *Nanoscale*, 2014, **6**, 6819-6827.
10. Z. Zheng, Y. Cheng, X. Yan, R. Wang and P. Zhang, *J. Mater. Chem. A*, 2014, **2**, 149-154.
11. J. Li, J. Wang, D. Wexler, D. Shi, J. Liang, H. Liu, S. Xiong and Y. Qian, *J. Mater. Chem. A*, 2013, **1**, 15292.
12. F. Fu, J. Li, Y. Yao, X. Qin, Y. Dou, H. Wang, J. Tsui, K. Y. Chan and M. Shao, *ACS Appl. Mater. Interfaces*, 2017, **9**, 16194-16201.
13. B. Wang, X.-Y. Lu and Y. Tang, *J. Mater. Chem. A*, 2015, **3**, 9689-9699.
14. J. Li, S. Xiong, X. Li and Y. Qian, *J. Mater. Chem.*, 2012, **22**, 23254.
15. Y. Jin, L. Wang, Y. Shang, J. Gao, J. Li and X. He, *Electrochimica Acta*, 2015, **151**, 109-117.
16. G. Zhang, L. Yu, H. B. Wu, H. E. Hoster and X. W. Lou, *Adv Mater*, 2012, **24**, 4609-4613.
17. J. Li, S. Xiong, Y. Liu, Z. Ju and Y. Qian, *ACS Appl Mater Interfaces*, 2013, **5**, 981-988.
18. H. Sun, G. Xin, T. Hu, M. Yu, D. Shao, X. Sun and J. Lian, *Nat.Commun.*, 2014, **5**, 4526.
19. M. Bijelić, X. Liu, Q. Sun, A. B. Djurišić, M. H. Xie, A. M. C. Ng, C. Suchomski, I. Djerdj, Ž. Skoko and J. Popović, *J. Mater. Chem. A*, 2015, **3**, 14759-14767.
20. L. Zhou, D. Zhao and X. W. Lou, *Adv. Mater.*, 2012, **24**, 745-748.
21. J. Li, S. Xiong, X. Li and Y. Qian, *Nanoscale*, 2013, **5**, 2045-2054.
22. L. Hu, H. Zhong, X. Zheng, Y. Huang, P. Zhang and Q. Chen, *Sci.Rep.*, 2012, **2**, 986.